Photoproduction of the ω Meson on the Proton at Large Momentum Transfer

M. Battaglieri,[1] M. Brunoldi,[1] R. De Vita,[1] J. M. Laget,[2] M. Osipenko,[1] M. Ripani,[1] M. Taiuti,[1] G. Adams,[26] M. J. Amaryan,[35] E. Anciant,[2] M. Anghinolfi,[1] D. S. Armstrong,[34] B. Asavapibhop,[20] G. Asryan,[35] G. Audit,[2] T. Auger,[2] H. Avakian,[31] S. Barrow,[11] K. Beard,[16] M. Bektasoglu,[24] B. L. Berman,[12] A. Bersani,[1] N. Bianchi,[15] A. S. Biselli,[26] S. Boiarinov,[14] S. Bouchigny,[13] R. Bradford,[5] D. Branford,[19] W. J. Briscoe,[12] W. K. Brooks,[31] V. D. Burkert,[31] J. R. Calarco,[21] G. P. Capitani,[15] D. S. Carman,[23] B. Carnahan,[6] A. Cazes,[29] C. Cetina,[12] P. L. Cole,[30,31] A. Coleman,[34] D. Cords,[31] P. Corvisiero,[1] D. Crabb,[33] H. Crannell,[6] J. P. Cummings,[26] E. DeSanctis,[15] P.V. Degtyarenko,[14] R. Demirchyan,[35] H. Denizli,[25] L. Dennis,[11] K.V. Dharmawardane,[24] K. S. Dhuga,[12] C. Djalali,[29] G. E. Dodge,[24] D. Doughty,[7] P. Dragovitsch,[11] M. Dugger,[4] S. Dytman,[25] M. Eckhause,[34] H. Egiyan,[31] K. S. Egiyan,[35] L. Elouadrhiri,[7] L. Farhi,[2] R. J. Feuerbach,[5] J. Ficenec,[32] T. A. Forest,[24] A. P. Freyberger,[31] V. Frolov,[26] H. Funsten,[34] S. J. Gaff,[9] M. Gai,[8] M. Garcon,[2] G. Gavalian,[21] S. Gilad,[18] G. P. Gilfoyle,[28] K. L. Giovanetti,[16] E. Golovach,[3] K. Griffioen,[34] M. Guidal,[13] M. Guillo,[29] L. Guo,[31] V. Gyurjyan,[31] C. Hadjidakis,[13] D. Hancock,[34] J. Hardie,[7] D. Heddle,[7] F.W. Hersman,[21] K. Hicks,[23] R. S. Hicks,[20] M. Holtrop,[21] C. E. Hyde-Wright,[24] M. M. Ito,[31] K. Joo,[31] J. H. Kelley,[9] M. Khandaker,[22] W. Kim,[17] A. Klein,[24] F. J. Klein,[6] A.V. Klimenko,[24] M. Klusman,[26] M. Kossov,[14] L. H. Kramer,[10,31] Y. Kuang,[34] S. E. Kuhn,[24] J. Lachniet,[5] D. Lawrence,[20] M. Lucas,[29] K. Lukashin,[31] R.W. Major,[28] J. J. Manak,[31] C. Marchand,[2] S. McAleer,[11] J. McCarthy,[33] J.W. C. McNabb,[5] B. A. Mecking,[31] M. D. Mestayer,[31] C. A. Meyer,[5] K. Mikhailov,[14] M. Mirazita,[15] R. Miskimen,[20] V. Mokeev,[3] S. Morrow,[13] M. U. Mozer,[23] V. Muccifora,[15] J. Mueller,[25] G. S. Mutchler,[27] J. Napolitano,[26] S. O. Nelson,[9] S. Niccolai,[12] B. B. Niczyporuk,[31] R. A. Niyazov,[24] M. Nozar,[31] J. T. O'Brien,[6] A. K. Opper,[23] G. Peterson,[20] S. A. Philips,[12] N. Pivnyuk,[14] D. Pocanic,[33] O. Pogorelko,[14] E. Polli,[15] B. M. Preedom,[29] J.W. Price,[26] D. Protopopescu,[21] L. M. Qin,[24] B. A. Raue,[10,31] A. R. Reolon,[15] G. Riccardi,[11] G. Ricco,[1] B. G. Ritchie,[4] F. Ronchetti,[15] P. Rossi,[15] D. Rowntree,[18] P. D. Rubin,[28] K. Sabourov,[9] C. Salgado,[22] V. Sapunenko,[1] R. A. Schumacher,[5] V. S. Serov,[14] A. Shafi,[12] Y. G. Sharabian,[35] J. Shaw,[20] A.V. Skabelin,[18] E. S. Smith,[31] T. Smith,[21] L. C. Smith,[33] D. I. Sober,[6] M. Spraker,[9] A. Stavinsky,[14] S. Stepanyan,[35] P. Stoler,[26] S. Taylor,[27] D. J. Tedeschi,[29] L. Todor,[5] U. Thoma,[31] R. Thompson,[25] M. F. Vineyard,[28] A.V. Vlassov,[14] K. Wang,[33] L. B. Weinstein,[24] H. Weller,[9] D. P. Weygand,[31] C. S. Whisnant,[29] E. Wolin,[31] M. Wood,[29] A. Yegneswaran,[31] J. Yun,[24] B. Zhang,[18] J. Zhao,[18] and Z. Zhou[18]

(CLAS Collaboration)

[1]*Istituto Nazionale di Fisica Nucleare, Sezione di Genova and Dipartimento di Fisica, Università di Genova, Genova, Italy 16146*
[2]*CEA-Saclay, Service de Physique Nucleaire, Gif-sur-Yvette, France 91191*
[3]*Moscow State University, Moscow, Russia 119899*
[4]*Arizona State University, Tempe, Arizona 85287-1504*
[5]*Carnegie Mellon University, Pittsburgh, Pennsylvania 15213*
[6]*Catholic University of America, Washington, D.C. 20064*
[7]*Christopher Newport University, Newport News, Virginia 23606*
[8]*University of Connecticut, Storrs, Connecticut 06269*
[9]*Duke University, Durham, North Carolina 27708-0305*
[10]*Florida International University, Miami, Florida 33199*
[11]*Florida State University, Tallahasee, Florida 32306*
[12]*The George Washington University, Washington, D.C. 20052*
[13]*Institut de Physique Nucleaire d'Orsay, IN2P3, BP 1, Orsay, France 91406*
[14]*Institute of Theoretical and Experimental Physics, Moscow, Russia, 117259*
[15]*Istituto Nazionale di Fisica Nucleare, Laboratori Nazionali di Frascati, Frascati, Italy 00044*
[16]*James Madison University, Harrisonburg, Virginia 22807*
[17]*Kyungpook National University, Taegu 702-701, South Korea*
[18]*Massachusetts Institute of Technology, Cambridge, Massachusetts 02139-4307*
[19]*University of Edinburgh, Edinburgh EH9 3JZ, United Kingdom*
[20]*University of Massachusetts, Amherst, Massachusetts 01003*
[21]*University of New Hampshire, Durham, New Hampshire 03824-3568*
[22]*Norfolk State University, Norfolk, Virginia 23504*
[23]*Ohio University, Athens, Ohio 45701*
[24]*Old Dominion University, Norfolk, Virginia 23529*
[25]*University of Pittsburgh, Pittsburgh, Pennsylvania 15260*
[26]*Rensselaer Polytechnic Institute, Troy, New York 12180-3590*

 0031-9007/03/90(2)/022002(5)$20.00 © 2003 The American Physical Society

[27]Rice University, Houston, Texas 77005-1892
[28]University of Richmond, Richmond, Virginia 23173
[29]University of South Carolina, Columbia, South Carolina 29208
[30]University of Texas at El Paso, El Paso, Texas 79968
[31]Thomas Jefferson National Accelerator Facility, Newport News, Virginia 23606
[32]Virginia Polytechnic Institute and State University, Blacksburg, Virginia 24061-0435
[33]University of Virginia, Charlottesville, Virginia 22901
[34]College of Willliam and Mary, Williamsburg, Virginia 23187-8795
[35]Yerevan Physics Institute, Yerevan, Armenia 375036
(Received 8 October 2002; published 16 January 2003)

The differential cross section, $d\sigma/dt$, for ω meson exclusive photoproduction on the proton above the resonance region ($2.6 < W < 2.9$ GeV) was measured up to a momentum transfer $-t = 5$ GeV^2 using the CLAS detector at Jefferson Laboratory. The ω channel was identified by detecting a proton and π^+ in the final state and using the missing mass technique. While the low momentum transfer region shows the typical diffractive pattern expected from Pomeron and Reggeon exchange, at large $-t$ the differential cross section has a flat behavior. This feature can be explained by introducing quark interchange processes in addition to the QCD-inspired two-gluon exchange.

DOI: 10.1103/PhysRevLett.90.022002 PACS numbers: 13.60.Le, 12.40.Nn, 13.40.Gp

In this Letter we report results of the first comprehensive measurement of the cross section for ω meson photoproduction on protons for E_γ between 3.19 and 3.91 GeV over the $-t$ range 0.1–5.0 GeV^2. Previous studies at Deutsches Elektronen-Synchrotron DESY, Stanford Linear Accelerator Center (SLAC), and NINA electron synchrotron (NINA) [1–3] are sparse and cover a limited kinematic range of $-t < 1$ GeV^2 [1,2] and $-t \sim -t_{\max}$ (4–5 GeV^2) [3]. The low momentum transfer data ($-t <$ 1 GeV^2) show a diffractive behavior that can be interpreted in the framework of the vector meson dominance (VMD) model [4] as the elastic scattering of vector mesons off the proton target. In a more recent approach, this process is also described by the t-channel exchange of the Pomeron and the dominating π Regge trajectory [5]. Other approaches [6,7] based on effective Lagrangians and inclusion of nucleon resonances as predicted by quark model calculations are able to reproduce the data at lower photon energies. At high $-t$, where the cross section is sensitive to the microscopic details of the interaction, the underlying physics can be described using parton degrees of freedom. The onset of this regime can be tested by a combined analysis of different flavor channels. The recent Jefferson Laboratory (JLab) measurements of ϕ [8] and ρ [9] photoproduction cross sections at large momentum transfer show a behavior consistent with a QCD-inspired framework [10–12]. At large $-t$, the small impact parameter ($\approx 1/\sqrt{-t}$) prevents the constituent gluons (quarks) of the exchange from interacting and forming a Pomeron (Reggeon). Because of the dominant $s\bar{s}$ component of the ϕ, quark exchange is strongly suppressed in this channel by the Okubo-Zweig-Iizuka rule and the two-gluon mechanism dominates [Figs. 1(a) and 1(b)] [5,11,13]. In contrast, the light quark composition of the ρ allows valence quarks to be exchanged between the baryon and the meson states [Fig. 1(c)] [5,12]. The same quark exchange mechanism is predicted to dominate the ω sector. Complete and detailed measurements of the ω differential cross section are therefore a stringent test of this conjecture.

The measurement was performed at Jefferson Laboratory with a bremsstrahlung photon beam produced by a continuous electron beam of $E_0 = 4.1$ GeV hitting a gold foil of 10^{-4} radiation lengths. A bremsstrahlung tagging system [14], with a photon energy resolution of 0.1% E_0, was used to tag photons in the energy range from 3–4 GeV. The target cell, a Mylar cylinder of 6 cm in diameter and 18 cm long, was filled with liquid hydrogen at 20.4 K. The high-intensity photon flux ($\sim 4 \times 10^6 \gamma$/s) was continuously monitored during data taking by an e^+e^- pair spectrometer located downstream of the target. The efficiency of this device was determined during dedicated low intensity ($\sim 10^5 \gamma$/s) runs by comparison with a 100% efficient lead-glass total absorption counter. The systematic uncertainty of the photon flux has been estimated to be 5%.

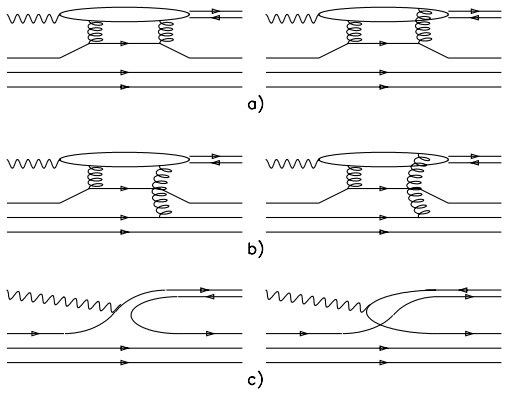

FIG. 1. The Feynman diagrams corresponding to (a) two-gluon exchange from a single quark, (b) two-gluon exchange taking into account quark correlations in the nucleon, and (c) quark exchange.

The hadrons were detected in CLAS (CEBAF Large Acceptance Spectrometer) [15], a spectrometer with nearly 4π coverage with a toroidal magnetic field (~ 1 T) generated by six superconducting coils. The field was set to bend the positive particles away from the beam into the acceptance of the detector. Three drift chamber regions allowed tracking of charged particles [16], and time-of-flight (TOF) scintillators were used for hadron identification [17]. The momentum resolution was of the order of a few percent, while the detector geometric acceptance was about 70% for positive hadrons. Low energy negative particles, however, were mainly lost at forward angles because they were bent out of the acceptance. Coincidences between the photon tagger and the CLAS detector (TOFs) triggered the recording of hadronic interactions. From a total of 70×10^6 triggers, 100×10^3 events were identified as $p\omega$ candidates.

For this analysis we chose the most sizable ω decay mode ($\omega \to \pi^+\pi^-\pi^0$, branching ratio 88.8%), requiring detection of both the proton and the π^+ in CLAS. The data analysis consisted of two main steps: two-pion background rejection and ω yield extraction from the multimeson background. Because of the different dynamics governing the low and the high $-t$ domains, we divided the data set into two samples corresponding to low ($-t < 1$ GeV^2) and high ($-t > 1$ GeV^2) momentum transfer. The analysis procedure was then performed and optimized independently for the two samples.

The two-pion background is dominated by the $\gamma p \to p\rho^0$ channel since its cross section is 5 times larger than that for $\gamma p \to p\omega$ for $E_\gamma \sim 3$–4 GeV, and the mass of the ρ meson (770 MeV) is very close to the ω mass (783 MeV). Even though the ρ has a larger width (~ 150 MeV FWHM) compared to the ω (~ 8 MeV FWHM enlarged to $\sim$55 MeV FWHM by the experimental resolution), the missing mass for the reaction $\gamma p \to pX$ alone does not allow separation of the two channels. The two-pion background was rejected by requiring that the missing mass for the reaction $\gamma p \to p\pi^+X$ be larger than 0.3 GeV. We estimated that the ω's surviving this cut were around 99%. Figure 2 shows the $(p\pi^+)$ missing mass squared spectrum: the missing π^- peak was easily removed (the hatched area corresponds to the retained events). The small contamination surviving the cut (estimated to be around 5% by the simulations) is spread over a wide proton missing mass interval, and it was reduced to a negligible level in the second step of the analysis. The ω yield extraction from the multimeson background was performed on the proton missing mass spectrum by using two different procedures: a Gaussian fit to the ω peak and a sideband subtraction.

Both of them rely on the hypothesis of a smooth and continuous background variation from one sideband region to the other. The two methods were not totally independent, but the comparison of their results allowed estimation of the systematic error related to the ω identification. The proton missing mass in each $-t$ bin was fitted to a Gaussian curve (the ω peak) plus a fourth order polynomial (the multimeson background). The ω yields in each $-t$ bin were the area under the Gaussian. Figure 3 shows the fitted spectra in a low and high $-t$ bin. The sideband subtraction procedure allowed extraction of a localized signal over an extended background subtracting the regions on either side of the peak (sidebands) after a proper normalization. The middle region was fixed at 6σ of the Gaussian curve describing the ω peak ($\sigma \sim 24$ MeV) while the sidebands had a width of 3σ each. The ω yield was obtained as the average of the two procedures while the maximum difference, 8%, was used as an estimate of the systematic error.

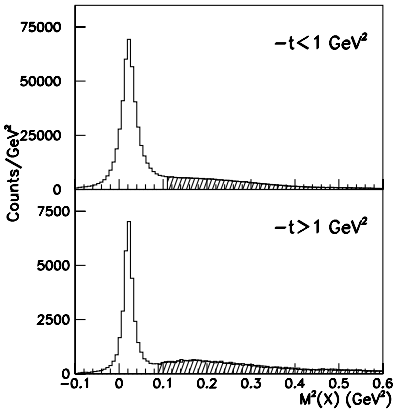

FIG. 2. Missing mass squared for the reaction $\gamma p \to p\pi^+X$ with E_γ between 3.19 and 3.91 GeV. The hatched area corresponds to the ω candidates.

The CLAS acceptance and reconstruction efficiency were evaluated with Monte Carlo simulations using the event generator of Ref. [18]. This code included the main contributions to the $p\pi^+\pi^-$ ($\gamma p \to p\rho^0$, $\gamma p \to \Delta^{++}\pi^-$, and $\gamma p \to p\pi^+\pi^-$ in s-wave) and $p\pi^+\pi^-\pi^0$ final states ($\gamma p \to p\omega$ and $\gamma p \to p\pi^+\pi^-\pi^0$ phase space), along

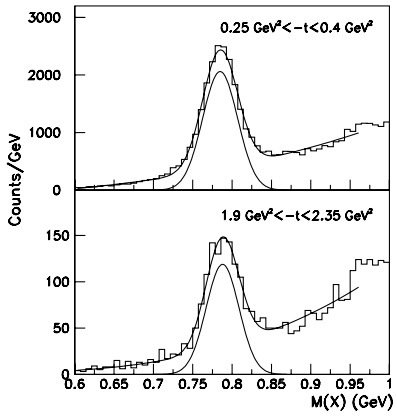

FIG. 3. Missing mass for $\gamma p \to p + X$ around the ω mass with E_γ between 3.74 and 3.92 GeV. The spectra are fitted to a Gaussian +4th-order polynomial.

with background reactions with four or more pions. The generated events were processed by a GEANT-based code simulating the CLAS detector, and reconstructed using the same analysis procedure that was applied to the raw data. The acceptance was derived as a function of E_γ and the momentum transfer t, integrating over the remaining independent variables. To minimize the model dependence in the acceptance calculation, the $\gamma p \to p\omega$ differential cross section was iteratively determined from the data and implemented in the Monte Carlo code. The final state (p and π^+ detected) did not allow us to measure the ω decay; therefore, the available experimental data about the decay matrix elements [1,2], as well as the general decay property of vector mesons [19], were implemented in the event generator. The systematic error associated with the efficiency calculation was estimated by comparing the results obtained after generating events with slightly different distributions both in production and decay. The resulting systematic uncertainty was estimated to be $\sim$10%. The average acceptance of CLAS for detected $p\pi^+$ ranged from 8% to 10%. For the very forward angles ($-t < 0.1$ GeV^2) and the very backward angles ($-t \sim -t_{\rm max}$) the CLAS detector had no acceptance for this reaction.

The ω photoproduction cross section as a function of t was extracted in four energy bins in the range 3.19–3.91 GeV. Data are shown in Figs. 4 and 5: vertical error bars include both the statistical uncertainties (ranging from 2% to 25%) and the overall systematic error (14%) summed in quadrature, while the horizontal bars reflect the bin sizes. In the low momentum transfer region, $0.1 < -t < 0.5$ GeV^2, good agreement with the previous measurement of Ref. [2] in a similar energy range is evident. At higher $-t$ the CLAS data lie between the two data sets taken, respectively, at smaller and larger energy. Assuming an exponential Ae^{Bt} behavior in the range $0.1 < -t < 0.5$ GeV^2, the coefficient resulting from this experiment, $B = 5.4 \pm 0.6$ GeV^{-2}, is consistent with the values $B = 5.1 \pm 1.4$ and $B = 7.1 \pm 1.7$ GeV^{-2} obtained by fitting, respectively, the $E_\gamma = 2.8$ GeV and $E_\gamma = 4.7$ GeV data sets reported in Ref. [2]. Good agreement is also found with existing data at the largest momentum transfer taken at NINA [3] with a bremsstrahlung photon beam and a single arm spectrometer.

Predictions of the QCD-inspired model of Refs. [5,12] are also shown in Fig. 4. Here the Pomeron exchange has been replaced by the exchange of two nonperturbatively dressed gluons (dotted line). The low momentum transfer region is dominated by the pion exchange that, added to the two-gluon and $f_2(1270)$ trajectory exchanges, gives good agreement up to $-t \sim 1$ GeV^2. The π exchange gives a strong contribution because of the large coupling constant $g_{\omega\pi\gamma}$ (0.334). Close to the upper kinematic limit ($-t \sim -t_{\rm max}$) the cross section is well reproduced by the exchange of the nucleon Regge trajectory in the u channel [20]. At intermediate momentum transfer, the two-gluon exchange contribution underestimates (by an order of magnitude) the experimental cross section. The calculation uses the same expression as in our phi-photoproduction work [5,8], where only the relevant mass

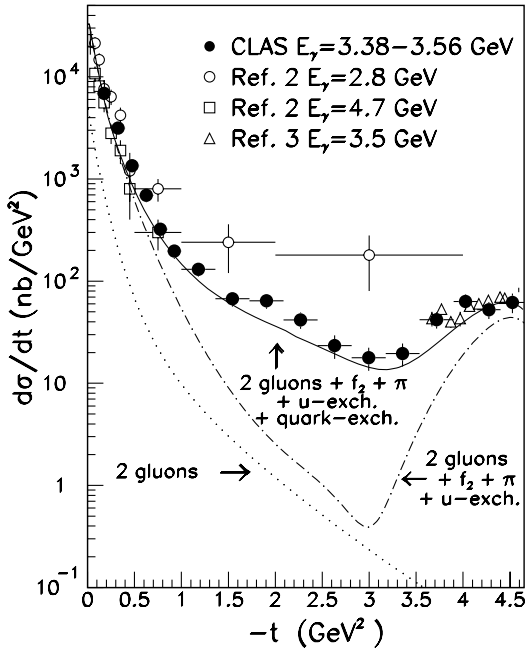

FIG. 4. Differential cross section for $\gamma p \to p\omega$ as measured in CLAS for the energy bin $E_\gamma = 3.38$–3.56 GeV compared with existing data. See the text for the explanation of the curves. In this energy bin, $\theta^*_\omega = 90°$ corresponds to $-t = 2.52$ GeV^2.

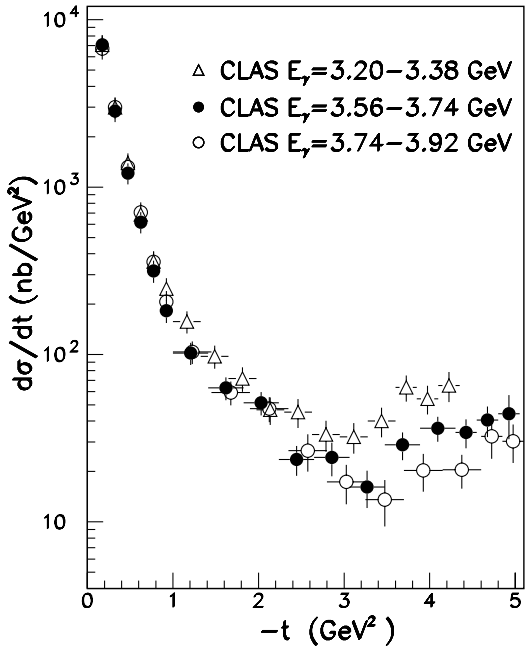

FIG. 5. Differential cross section measured in CLAS. The fourth energy bin ($E_\gamma = 3.38$– – 3.56 GeV) is shown in Fig. 4.

and radiative decay width have been changed. In contrast to the ϕ meson, quark interchanges [Fig. 1(c)] are not forbidden in ω production. As explained in Refs. [20,21] these hard-scattering mechanisms can be incorporated in an effective way by using the so-called "saturated" trajectory that is independent of t at large momentum transfer [22]. Regge trajectories are usually assumed to be linear in t, but there are both phenomenological and theoretical arguments supporting the idea of nonlinear trajectories [23]. Saturated trajectories lead to the asymptotic quark counting rules [24] that, model independently, determine the energy behavior of the cross section at large $-t$. This approach was successfully adopted to explain the large momentum transfer hadron-hadron interactions [25–27], as well as several photon-induced reactions [9,20,28]. The pion saturating trajectory [$\alpha_\pi^{\rm sat}(t) \to -1$ when $-t \to -\infty$] is in a form that reproduces the $\gamma p \to n\pi^+$ reaction around $\theta_\omega^* = 90°$ [20]. The solid line in Fig. 4 shows the full calculation, including such a saturating trajectory, while the dot-dashed line corresponds to the same calculation with linear trajectories. Quark exchange increases the cross section at large $-t$ by more than 1 order of magnitude.

The measured $d\sigma/dt$ in the other three photon energy bins are shown in Fig. 5. From the four data sets, the cross section at $\theta_\omega^* = 90°$ was extracted as a function of energy. A power-law fit s^{-C} to $d\sigma/dt$ at $\theta_\omega^* = 90°$ was performed also using the only other datum available in the literature (SLAC datum at $s = 6.13$ GeV^2 [2]). The experimental points include both statistical and systematic errors summed in quadrature. The fit yields $C = 7.2 \pm 0.7$ ($\chi^2 = 0.5$). It is the first time that such a power-law behavior, seen for other exclusive reactions [2,28], has been observed in the ω channel. The quark exchange diagrams of Fig. 1(c) (left) (pointlike interaction) and 1(c) (right) (hadronic component of the photon) have a s^{-7} and a s^{-8} power-law behavior, respectively, both in dimensional counting [24] and in recent models [29]. Note that the saturated π Regge trajectory behaves like s^{-8}, too. Besides the differential cross section at fixed energy, the s dependence is a strong hint of the presence of quark interchange hard mechanisms in addition to the two-gluon exchange process.

In conclusion, elastic photoproduction of the ω mesons from the proton was measured for the first time with nearly complete kinematic coverage. The energy power-law behavior of the differential cross section at $\theta_\omega^* = 90°$ was observed. The comparison with a QCD-inspired model, able to reproduce the ϕ and the ρ^0 photoproduction data, provides further evidence for the presence of hard processes. Adopting a QCD language in this energy region, the two-gluon exchange mechanism (that fully describes the ϕ photoproduction data) badly misses the cross section at large momentum transfer and its energy dependence. Good agreement is achieved when quark interchange processes, suppressed in the ϕ channel and weakly contributing in the ρ case, are included in an effective way in the calculation of the ω cross section.

We acknowledge the outstanding efforts of the staff of the Accelerator and the Physics Divisions at JLab that made this experiment possible. This work was supported in part by the Italian Istituto Nazionale di Fisica Nucleare, the French Centre National de la Recherche Scientifique and the Commissariat à l'Energie Atomique, the U.S. Department of Energy and the National Science Foundation, and the Korea Science and Engineering Foundation. The Southeastern Universities Research Association (SURA) operates the Thomas Jefferson National Accelerator Facility for the United States Department of Energy under Contract No. DE-AC05-84ER40150.

[1] ABBHHM Collaboration, Phys. Rev. **175**, 1669 (1968).
[2] J. Ballam *et al.*, Phys. Rev. D **7**, 3150 (1973).
[3] R.W. Clifft *et al.*, Phys. Lett. **72B**, 144 (1977).
[4] T. H. Bauer *et al.*, Rev. Mod. Phys. **50**, 261 (1978).
[5] J. M. Laget, Phys. Lett. B **489**, 313 (2000).
[6] B. Friman and M. Soyeur, Nucl. Phys. **A600**, 477 (1996).
[7] Y. Oh *et al.*, Phys. Rev. C **63**, 025201 (2001).
[8] E. Anciant *et al.*, Phys. Rev. Lett. **85**, 4682 (2000).
[9] M. Battaglieri *et al.*, Phys. Rev. Lett. **87**, 172002 (2001).
[10] A. Donnachie and P.V. Landshoff, Phys. Lett. B **185**, 403 (1987).
[11] J. M. Laget and R. Mendez-Galain, Nucl. Phys. **A581**, 397 (1995).
[12] F. Cano and J. M. Laget, Phys. Rev. D **65**, 074022 (2002).
[13] J. M. Laget, in *Physics and Instrumentation with 6–12 GeV Beams*, edited by S. Dytman, H. Fenker, and P. Ross (Jefferson Lab User Production, Newport News, VA, 1998), p. 57.
[14] D. I. Sober *et al.*, Nucl. Instrum. Methods Phys. Res., Sect. A **440**, 263 (2000).
[15] W. Brooks, Nucl. Phys. **A663–A664**, 1077 (2000).
[16] M. D. Mestayer *et al.*, Nucl. Instrum. Methods Phys. Res., Sect. A **449**, 81 (2000).
[17] E. S. Smith *et al.*, Nucl. Instrum. Methods Phys. Res., Sect. A **432**, 265 (1999).
[18] P. Corvisiero *et al.*, Nucl. Instrum. Methods Phys. Res., Sect. A **346**, 433 (1994).
[19] M. Stevenson *et al.*, Phys. Rev. **125**, 687 (1961).
[20] M. Guidal, J. M. Laget, and M. Vanderhaeghen, Nucl. Phys. **A627**, 645 (1997).
[21] P. D. B. Collins and P. J. Kearney, Z. Phys. C **22**, 277 (1984).
[22] M. N. Sergeenko, Z. Phys. C **64**, 315 (1994).
[23] M. Brisudova *et al.*, Phys. Rev. D **61**, 054013 (2000).
[24] S. J. Brodsky and G. R. Farrar, Phys. Rev. Lett. **31**, 1153 (1973).
[25] D. D. Coon *et al.*, Phys. Rev. D **18**, 1451 (1978).
[26] R. Fiore *et al.*, Phys. Rev. D **60**, 116003 (1999).
[27] C. White *et al.*, Phys. Rev. D **49**, 58 (1994).
[28] M. Shupe *et al.*, Phys. Rev. D **19**, 1921 (1979).
[29] H.W. Huang and P. Kroll, Eur. Phys. J. C **17**, 423 (2000).